Publisher: GSA
Journal: GEOL: Geology
DOI:10.1130/G37870.1

Simultaneous eruptions from multiple vents at Campi Flegrei (Italy) highlight new eruption processes at calderas

Marco Pistolesi[1], Roberto Isaia[2], Paola Marianelli[3], Antonella Bertagnini[4], Céline Fourmentraux[3], Paul G. Albert[5], Emma L. Tomlinson[6], Martin A. Menzies[7], Mauro Rosi[3] and Alessandro Sbrana[3]

[1]*Dipartimento di Scienze della Terra, Università di Firenze, via G. La Pira 4, Florence, Italy*

[2]*Istituto Nazionale di Geofisica e Vucanologia, via Diocleziano 328, Naples, Italy*

[3]*Dipartimento di Scienze della Terra, Università di Pisa, via S. Maria 53, Pisa, Italy*

[4]*Istituto Nazionale di Geofisica e Vucanologia, via della Faggiola 32, Pisa, Italy*

[5]*Research Laboratory for Archaeology and the History of Art, University of Oxford, Dyson Perrins Building, South Parks Road, Oxford, OX1 3QY, UK*

[6]*Department of Geology, Trinity College Dublin, Dublin 2, Ireland*

[7]*Department of Earth Sciences, Royal Holloway University of London, Egham, Surrey, TW20 0EX, UK*

ABSTRACT

Volcanic eruptions are typically characterized by the rise and discharge of magma at the surface through a single conduit/vent system. However, in some cases, the rise of magma can be triggered by the activation of eruptive fissures and/or vents located several kilometers apart. Simultaneous eruptions from multiple vents at calderas, not related to caldera collapse (e.g., ring faults) are traditionally regarded as an unusual phenomenon, the only historically reported examples occurring at Rabaul caldera, Papua New Guinea.

Multiple venting within a caldera system is inherently difficult to demonstrate, owing partly to the infrequency of such eruptions and to the difficulty of documenting them in time and space.

We present the first geological evidence that at 4.3 kyr ago the Solfatara and Averno vents, 5.4 km apart, erupted simultaneously in what is now the densely populated Campi Flegrei caldera (Southern Italy). Using tephrostratigraphy and geochemical fingerprinting of tephras, we demonstrate that the eruptions began almost at the same time and alternated with phases of variable intensity and magnitude. The results of this study demonstrate that multi-vent activity at calderas could be more frequent than previously thought and volcanic hazards could be greater than previously evaluated. More generally we infer that the simultaneous rise of magma and gas along different pathways (multiple decrepitation of chamber/s) could result in a sudden pressure rise within sub-caldera magmatic system.

INTRODUCTION

The forecasting of future eruptive vent locations is a challenging goal in volcanology and an important element in the volcanic emergency arrangements. Most calderas have produced highly explosive and effusive eruptions from widespread vents that are difficult to reconcile to any regular spatio-temporal pattern (Bosworth et al., 2003; Acocella, 2007; Cashman and Giordano, 2014). Although multi-vent activity has been described at several volcanic centers worldwide during fissure-fed eruptions (e.g., Walker et al., 1984; Smith et al., 2006), the possibility of simultaneous, or quasi-contemporaneous, eruptions from independent vents within caldera systems has rarely been reported. To date, Rabaul caldera (Papua New Guinea) showed this phenomenon on three occasions - 1878, 1937, 1994 (Roggensack et al., 1996). This raises a question as to whether multi-vent activity is a peculiarity of this specific volcanic system, or if such behavior has occurred at other calderas worldwide. The twin eruptions of 1994 at Rabaul caldera were preceded by volcano-seismic and deformation crises in 1983 and 1985 (McKee et al., 1984). At Campi Flegrei caldera (Southern Italy), a very similar crisis occurred in the mid-1980's but has not yet resulted in an explosive event. During detailed mapping for the new geological map of Naples 446–447 sheets (ISPRA CAR.G Project, Italy), interlayered pyroclastic deposits of the Averno and Solfatara volcanoes were reported within the Campi Flegrei caldera (Isaia et al., 2009). This paper presents a detailed stratigraphic reconstruction and geochemical study of the juvenile component of these pyroclastic deposits and aims to unravel and document the relative timing of the "simultaneous" eruptions from the Solfatara and Averno volcanoes at 4.3 ka BP. The robust documentation of the coeval Averno and Solfatara eruptions can shed light on the potential eruptive behavior of calderas worldwide. Multi-vent activity could actually be more common than previously envisaged even for lower intensity eruptions unrelated to caldera formation.

THE AVERNO 2 AND SOLFATARA ERUPTIONS

The Campi Flegrei caldera (CFc) is one of the most active caldera systems on Earth. In recent decades, CFc has exhibited significant deformation in its central sector, with uplift of several meters centered on the town of Pozzuoli (Del Gaudio et al., 2010). In January 2013, based on very recent ground uplift episodes and gas chemistry data, the Dipartimento della Protezione Civile (Italy) raised the state of CFc from the green (quiet) to the yellow (scientific attention) level. The dense urbanization of the region, where more than three hundred thousand people live within the caldera, makes the volcanic risk at CFc one of the highest in the world.

The present structure of the CFc (Vitale and Isaia, 2014) results from a main collapse related to the eruption of the Campanian Ignimbrite (CI) at ca. 40 ka (Rosi and Sbrana, 1987; Orsi et al., 1996) and from minor collapses linked to the Neapolitan Yellow Tuff (NYT) eruption at ca. 15 ka (Orsi et al., 1992).

The Averno 2 eruption (4181 – 4386 yr B.P.; Isaia et al., 2009; Smith et al., 2011), or simply the Averno eruption according to the nomenclature introduced by the recent geological map (ISPRA CAR.G Project), occurred in the western sector of the CFc. It was characterized by repeated episodes of sustained and collapsing columns that generated a complex sequence of pumice fall and pyroclastic density currents (PDCs) deposits with a total volume of 0.07 km^3. The tephra sequence has been divided (Di Vito et al., 2011) into three members, from base to top, A, B and C. Member A has been subdivided into six fallout sub-members (A0 to A5) interlayered with thin, fine-grained surge deposits. Members B and C consist mainly of surge bedsets intercalated with minor fallout deposits. The whole nomenclature of tephra layers is detailed in the Data Repository. According to Di Vito et al. (2011), the highest intensity of the eruption was reached during emplacement of the A2 sub-Member, with an estimated column height of 10 km. The Averno 2 eruption was fed by two trachytic and shallow (<4 km) magma batches with slightly differing degrees of evolution and geochemical signature (Di Vito et al., 2011; Fourmentraux et al., 2012). The most evolved end-member was discharged during the initial phase (A0) and the least evolved in the final part of the eruption (C). Systematic analyses of matrix glass of juvenile pumice fragments show that glasses of the upper part of the fallout deposit A2 (A2t) and of the member B (Bt) are strongly heterogeneous (mingled) with compositions covering the entire compositional range between the two endmembers A0 and C (Fourmentraux et al., 2012). Hereafter, for simplicity, we divide the Averno 2 eruption into three main phases: i) opening phase (corresponding to Member A0 of Di Vito et al., 2011), fed by a more evolved compositional end-member; ii) intermediate phase, which includes the peak fallout deposit (A2t) followed by PDC and minor fallout deposits (member B); iii) final phase (PDC and minor fallout deposits of Member C), containing the less evolved compositional end-member.

The Solfatara eruption (4181 - 4386 yr B.P.; Isaia et al., 2009; Smith et al., 2011; Isaia et al., 2015) occurred in the central-eastern sector of the CFc, 5.4 km from Averno lake (Figs. DR1 and DR2). The tephra sequence consists of an opening, mainly phreatic phase. This comprises massive to crudely stratified, fine to coarse ash and block deposits containing scarce juvenile material and minor stratified PDC deposits with limited dispersal. Later in the eruption, shallow discrete Vulcanian explosions produced low eruption columns emplacing accretionary lapilli-bearing ash fallout deposits and PDCs distributed around the Solfatara crater. This phase of the Solfatara eruption was fed by a homogeneous trachytic magma batch stored at shallow (<3 km) level (Cipriani et al., 2008).

STRATIGRAPHY AND SEDIMENTOLOGY

We present data for a well-preserved, key stratigraphic section where deposits of two eruptions are interlayered (Isaia et al., 2009). The outcrop is ~2 km northwest of Solfatara crater and 4 km northeast of Averno lake (Fig. DR1). The section is separated by a thick (>15 cm) paleosol from the underlying deposits of the Agnano Monte Spina eruption (4482 – 4625 yr B.P.; Smith et al., 2011) and by an upper, 3-cm-thick humified horizon from ash beds belonging to the Astroni volcano (4098 – 4297 yr B.P.; Isaia et al., 2004) (Fig. 1a, b).

The succession is 100 cm-thick and consists of alternating greenish to light gray ash beds containing accretionary lapilli (Fig. 1). Light colored and white coarser ash beds with scattered pumice clasts are interlayered at various heights. The section has been subdivided into 5 main units, mainly based on tephra sedimentological characteristics (color and grain-size variations), consisting of an alternation of accretionary lapilli-bearing, ash layers with scattered pumice fragments. Each unit is presented and described in detail in Figure DR3. The stratigraphic log, sample location and results of grain-size analyses are presented in Figure DR4, and all the analytical methodologies are detailed in the Data Repository.

MAJOR AND TRACE ELEMENT GLASS COMPOSITIONS

About 140 juvenile clasts were analyzed from the tephra sequence (Table DR1). Glass analyses were obtained for 13 lapilli-sized clasts (from 2 to 6 cm) and one bomb (10 cm) at the base of Unit 1 (sample SA1), pumice fragments from light colored tephra beds of Units 2 (SA3), 4 (SA17), and 5 (SA19), fine white ash from accretionary lapilli in Unit 3 (SA11) and 4 (SA12) and pumice fragments from the greenish deposits of Unit 3 (SA5, SA9) and 4 (SA18). The data were compared to those already obtained by Cipriani et al. (2008) for the products of Solfatara and by Fourmentraux et al. (2012) for those of Averno 2.

Glassy groundmass pumice collected in the green ash layers of Units 3 and 4 (SA5, SA9 and SA18) show a fairly homogeneous trachytic composition (SiO_2 = 59.3–60.8 wt.%, CaO = 2.1–3.0 wt.%, Na_2O 3.9–5.4 wt.%, K_2O = 8.0–9.0 wt.%) perfectly matching the composition of the Solfatara products (Cipriani et al., 2008). Samples belonging to the light colored layers show a wider compositional range (SiO_2 = 59.0–63.3 wt.%, CaO = 1.5–2.5 wt.%, Na_2O4.6–6.8 wt.%, K_2O = 6.6 = 8.7 wt.%). This range encompasses all the variability of Averno 2 glasses and extends to compositions clearly distinct from Solfatara samples, which have higher contents of CaO, Al_2O_3, FeO and K_2O and lower contents of SiO_2 and Na_2O. Glassy groundmass pumice clasts from Units 1 (SA1), 2 and 3 and the base of Unit 4 (SA3, SA11 and SA12) have heterogeneous compositions covering the entire range of the Averno 2 sequence, essentially comparable to those of the intermediate phase (Fig. 2) (Fourmentraux et al., 2012). In constrast, glasses from the top of the sequence (SA17 and SA19 from Units 4 and 5) show a more homogeneous and less evolved composition (K_2O = 8.1 ± 0.2 wt.%) (Fig. 2 and Table DR1), similar to the less evolved trachytic end member emitted during the final phase of Averno 2 eruption. Accretionary lapilli from the upper part of Unit 3 have cores formed by white ash chemically identical to the Averno compositions and green ash coatings with the composition of Solfatara juvenile fraction.

To further constrain the major element geochemistry, a total of 70 trace element analyses were performed on 8 selected samples (SA1, SA3, SA5, SA9, SA12, SA17, SA18, SA19). Representative samples of Solfatara (SF12_4) and of the two end-members emitted during the opening (A0) and final (Cmb) phase of Averno eruptions were also analyzed for comparison (Table DR2). Despite the overlap of some incompatible trace elements with the final phase products of the Averno 2 eruption (e.g., Th, Nb, Zr), Solfatara glasses clearly differ from Averno glasses by having markedly higher Ba and Sr contents (Fig. 3, Table DR2). Only one clast of Solfatara shows lower Sr and Ba contents possibly due to K-feldspar crystallization in the matrix glass. Trace elements confirm the heterogenous compositions of Units 1, 2, and the base of Unit 4 (SA12) and more homogeneous compositions close to the final phase of Averno 2 eruption in Units 4 (SA17 and SA19) (Fig. 3).

TEPHRA CORRELATIONS

Detailed sedimentological and chemical analyses performed on the key tephra sequence allow us to attribute the green ash beds to Solfatara and the light colored beds to the Averno 2 eruption. Dispersal and grain-size analyses of greenish deposits are consistent with a medial deposit which recorded the main stages of the Solfatara eruption. In particular, Unit 1, including a scarce juvenile component, represents the basal Solfatara stratified deposits emplaced during the opening phase. The fairly homogeneous composition of the juvenile glassy groundmass from Units 3 and 4 matches that of Solfatara products, thus indicating a correlation to the second phase of the Solfatara eruption.

The light colored ash to lapilli-size clasts and whitish to pink layers intercalated within the green ash sequence reveal a larger, more evolved compositional range that matches the different phases of the Averno 2 eruption. Major and trace element contents of lapilli and bomb-sized clasts embedded within Unit 1 (SA1 sample) agree with the composition of the top of A2 fallout deposit, corresponding to the climax of Averno 2. The whole of Unit 2 (SA3), and lapilli from the upper part of the Unit 3 (SA11), and from

Unit 4 (SA12) record the PDC-dominated phase of the Averno 2 eruption (intermediate phase). Finally, the chemical composition of lapilli from the upper part of Unit 4 (SA17) and Unit 5 (SA19) correlate well with the glass chemistry of the final phase of Averno 2.

TIMING AND ERUPTIVE DYNAMICS

The correlation of the deposits in the key section with the different phases of the two eruptions allows us to make inferences about the timing of the two contemporaneous eruptive events (Table DR3). Unit 1 records the beginning of the Solfatara eruption; ash deposits are thin at the studied site and thicken toward the Solfatara crater, where phreatic breccias are present at the crater rim. Also at this stage, magmatic explosions and sustained eruptive columns started at the Averno 2 vent; pumice bombs and lapilli produced during the sub-Plinian climactic phase are interlayered within Unit 1. Stratigraphic studies of other outcrops indicate that the pumice clast size and thickness of the fallout deposit increase toward the Averno 2 crater. Unit 2 probably records either a pause in the Solfatara activity or a shift in wind direction, during which time the Averno 2 eruptive plume, characterized by ash-laden plumes related to PDCs during its intermediate phase, drifted northeastward. Afterward, a new wind shift or a resumption of the Solfatara activity with magmatic and possibly phreatomagmatic, Vulcanian-type explosions, emplaced breccia deposits and roughly stratified ashes (Unit 3). In the basal part of Unit 3, the Averno 2 products are recorded only by the light ash coatings on the green accretionary lapilli. In the upper part of Unit 3, “inverse” accretionary lapilli, with cores of light ash chemically identical to Averno 2 and coatings of green ash with the composition of Solfatara juvenile clasts occur. The alternation of normal and “inverse” accretionary lapilli suggest either a downturn in activity from one vent and/or a higher

DOI:10.1130/G37870.1

sedimentation rate of ash from the other, which forms the cores of the accretionary lapilli. In addition, the cores of accretionary lapilli possibly formed higher in the atmosphere, where only Solfatara or Averno 2 ashes was present, and then fell into an eruptive cloud dominated by ash from the other eruption. If so, the zoning in the accretionary lapilli (both the normal and the “inverse” zoning) may reflect relative heights of the ash cloud from the two synchronous eruptions. Unit 4 is characterized by a close interlayering of green and light-colored ash beds related to ash fallout from Solfatara and to minor pumice fallout associated with PDCs in the final phase of Averno 2. This activity produced a rapid series of short-lived explosions, as shown by the proximal deposits of Averno 2 (Di Vito et al., 2011). Finally, the uppermost Unit 5 records only Averno 2 activity.

CONCLUDING REMARKS

This detailed study of the stratigraphy and geochemistry of an intra-caldera tephra sequence reveals that the two eruptions of Solfatara and Averno 2 evolved in parallel, despite coming from vents 5 km apart and located in sectors of the CFc characterised by different magma compositions, structural alignments and eruptive styles.

The compositional features of erupted products suggest the involvement of magmas tapped from different shallow portions of the whole Campi Flegrei magmatic system which evolved independently; however, the simultaneity of eruptive activity implies some form of connectivity to a common source at a deeper level. We speculate that the perturbation to the system triggering the two eruptions originated from this common deep reservoir. Since no evidence of arrival of mafic magmas have been detected, we also speculate that the trigger consisted in a sudden pressure increase within the magmatic system possibly due to volatiles saturation (Stock et al., 2016), which in turn caused the multiple decrepitation of its shallowest apophyses. It is worth noticing that most of the activity driven by phreatic/ash emission occurred at Solfatara, which is still the preferential path for gas emission of the caldera. This behaviour of contrasting activity remarkably resembles that of Rabaul 1994 eruption, which was mostly characterized by magma-driven explosivity (Vulcan) with contemporaneous emission of hydrothermally-altered material (Tavurvur) (Global Volcanism Program, 1994).

Moreover, the 1994 Rabaul eruption was preceded by a general uplift started years before, but the short-term precursory activity excalated only tens of hours before, with strong and shallow earthquakes, implying a rapid rise of gas and magma. If we assume a similar mechanism, we potentually expect the same scenario for the Averno-Solfatara event. The activation at both Rabaul and Campi Flegrei of the area of higher fluids discharge of the calderas (Tavurvur and Solfatara) also suggests that the destabilization of the magmatic reservoir could be promoted by the sudden rise of high-pressure gas masses, along the plumbing system feeding the shallow magma chamber/s.

Finally, the past occurrence of such eruptive dynamics has to be taken into account when assessing future volcanic hazards and considering a realistic eruptive scenario in case of future reactivation of calderas. This is particularly true for densely urbanized areas like CFc, which encompasses large parts of the cities of Pozzuoli and Naples.

ACKNOWLEDGMENTS

Financial support was provided by the projects “V1” and “Speed” funded by Dipartimento della Protezione Civile (Italy) and Regione Campania, and by ISPRA Regione Campania CAR.G Project 446–447 Napoli sheets. This research was partially funded by the NERC "RESET" consortium (NE/E015905/1) and forms "RHOXTOR" contribution 047. D. Swanson, K. Cashman and S. de Silva are greatly aknowledged for their insightful comments.

REFERENCES CITED

Acocella, V., 2007, Understanding caldera structure and development: An overview of analogue models compared to natural calderas: Earth-Science Reviews, v. 85, p. 125–160, doi:10.1016/j.earscirev.2007.08.004.

Bosworth, W., Burke, K., and Strecker, M., 2003, Effect of stress fields on magma chamber stability and the formation of collapse calderas: Tectonics, v. 22, p. n/a, doi:10.1029/2002TC001369.

Cashman, K.V., and Giordano, G., 2014, Calderas and Magma Reservoirs: Journal of Volcanology and Geothermal Research, v. 288, p. 28–45, doi:10.1016/j.jvolgeores.2014.09.007.

Cipriani, F., Marianelli, P., and Sbrana, A., 2008, Studio di una sequenza piroclastica del vulcano della Solfatara (Campi Flegrei): Atti Società Toscana Scienze Naturali Memorie, Serie A, v. 113, p. 1–6.

Del Gaudio, C., Aquino, I., Ricciardi, G.P., Ricco, C., and Scandone, R., 2010, Unrest episodes at Campi Flegrei: A reconstruction of vertical ground movements during 1905–2009: Journal of Volcanology and Geothermal Research, v. 195, p. 48–56, doi:10.1016/j.jvolgeores.2010.05.014.

Di Vito, M.A., Arienzo, I., Braia, G., Civetta, L., D'Antonio, M., Di Renzo, V., and Orsi, G., 2011, The Averno 2 fissure eruption: a recent small-size explosive event at the

Campi Flegrei Caldera (Italy): Bulletin of Volcanology, v. 73, p. 295–320, doi:10.1007/s00445-010-0417-0.

Fourmentraux, C., Métrich, N., Bertagnini, A., and Rosi, M., 2012, Crystal fractionation, magma step ascent, and syn-eruptive mingling: The Averno 2 eruption (Campi Flegrei, Italy): Contributions to Mineralogy and Petrology, v. 163, p. 1121–1137, doi:10.1007/s00410-012-0720-1.

Global Volcanism Program, 1994, Report on Rabaul (Papua New Guinea). In: Venzke, E (ed.), Bulletin of the Global Volcanism Network, 19:9. Smithsonian Institution. http://dx.doi.org/10.5479/si.GVP.BGVN199409-252140.

Isaia, R., D'Antonio, M., Dell'Erba, F., Di Vito, M., and Orsi, G., 2004, The Astroni volcano: The only example of closely spaced eruptions in the same vent area during the recent history of the Campi Flegrei caldera (Italy): Journal of Volcanology and Geothermal Research, v. 133, p. 171–192, doi:10.1016/S0377-0273(03)00397-4.

Isaia, R., Marianelli, P., and Sbrana, S., 2009, Caldera unrest prior to intense volcanism in Campi Flegrei (Italy) at 4.0 ka B.P: implications for caldera dynamics and future eruptive scenarios: Geophysical Research Letters, v. 36, p. L21303, doi:10.1029/2009GL040513.

Isaia, R., Vitale, S., Di Giuseppe, M.G., Iannuzzi, E., Tramparulo, F., and Troiano, A., 2015, Stratigraphy, structure and volcano-tectonic evolution of Solfatara maar-diatreme (Campi Flegrei, Italy): Geological Society of America Bulletin, v. 127, p. 1485–1504, doi:10.1130/B31183.1.

McKee, C.O., Lowenstein, P.L., de Saint Ours, P., Talai, B., Itikarai, I., and Mori, J.J., 1984, Seismic and ground deformation crises at Rabaul caldera: Prelude to an eruption?: Bulletin of Volcanology, v. 47, p. 397–411, doi:10.1007/BF01961569.

Orsi, G., D'Antonio, M., De Vita, S., and Gallo, G., 1992, The Neapolitan Yellow Tuff, a large-magnitude trachytic phreatoplinian eruption; eruptive dynamics, magma withdrawal and caldera collapse: Journal of Volcanology and Geothermal Research, v. 53, p. 275–287, doi:10.1016/0377-0273(92)90086-S.

Orsi, G., de Vita, S., and Di Vito, M., 1996, The restless, resurgent Campi Flegrei nested caldera (Italy): Constraints on its evolution and configuration: Journal of Volcanology and Geothermal Research, v. 74, p. 179–214, doi:10.1016/S0377-0273(96)00063-7.

Roggensack, K., Williams, S.N., Schaefer, S.J., and Parnell, R.A., 1996, Volatiles from the 1994 eruptions of Rabaul: Understanding large caldera systems: Science, v. 273, p. 490–493, doi:10.1126/science.273.5274.490.

Rosi, M., and Sbrana, A., 1987, The Phlegraean fields: CNR, Quaderni Ricerca Scientifica, v. 114, 175 p.

Smith, V.C., Shane, P., Nairn, I.A., and Williams, C.M., 2006, Geochemistry and magmatic properties of eruption episodes from Haroharo linear vent zone, Okataina Volcanic Centre, New Zealand during the last 10 kyr: Bulletin of Volcanology, v. 69, p. 57–88, doi:10.1007/s00445-006-0056-7.

Smith, V.C., Isaia, R., and Pearce, N.J.G., 2011, Tephrostratigraphy and glass compositions of post-15 kyr Campi Flegrei eruptions: implications for eruption history and chronostratigraphic markers: Quaternary Science Reviews, v. 30, p. 3638–3660, doi:10.1016/j.quascirev.2011.07.012.

Stock, M.J., Humphreys, M.C.S., Smith, V.C., Isaia, R. and Pyle, D.M., 2016, Late-stage volatile saturation as a potential trigger for explosive volcanic eruptions. Nature Geoscience, v. 9, p. 249-254, doi:10.1038/ngeo2639.

Vitale, S., and Isaia, R., 2014, Fractures and faults in volcanic rocks (Campi Flegrei, southern Italy): Insight into volcano-tectonic processes: International Journal of Earth Sciences, v. 103, p. 801–819, doi:10.1007/s00531-013-0979-0.

Walker, G.P.L., Self, S., and Wilson, L., 1984, Tarawera, 1886, New Zealand: A basaltic plinian fissure eruption: Journal of Volcanology and Geothermal Research, v. 21, p. 61–78, doi:10.1016/0377-0273(84)90016-7.

FIGURE CAPTIONS

Figure 1. (A) Key section where Solfatara and Averno 2 deposits are interlayered; (B) Unit 1: thin yellowish ash laminae intercalated with Solfatara tephra (greenish in color); (C) pisolitic ash layer from Unit 3; note that pisolites have a greenish core and yellowish rim; (D) pisolitic ash layer from the top of Unit 3 (sample SA11); note that pisolites have a yellowish core and a greenish rim; (E) detail of Unit 4. Locations of C-E shown in A.

Figure 2. Stratigraphic section of the Solfatara deposits showing plots of K_2O versus Na_2O (black diamonds, Solfatara samples; squares, circles, crosses and triangles refer to Averno 2 samples. Same symbols for Averno 2 refer to the same stratigraphic unit). The

DOI:10.1130/G37870.1

Solfatara field is from Cipriani et al. (2008); the three variability fields of Averno 2 are from Fourmentraux et al. (2012).

Figure 3. Ba/Th, Sr/Th and Th/Zr plots. Full colored symbols (stars, squares and triangles) refer to the reference clasts from Solfatara (SF12_4, green stars) and Averno 2 eruptions (A0 and Cmb, yellow triangles and squares, respectively). Analyses from the Averno 2 glasses represent the two compositional end-members of the opening (A0) and final (Cmb) phases. Error bars are within the symbols.

[1]GSA Data Repository item 2015xxx, xxxxxxxx, is available online at www.geosociety.org/pubs/ft2015.htm, or on request from editing@geosociety.org or Documents Secretary, GSA, P.O. Box 9140, Boulder, CO 80301, USA.

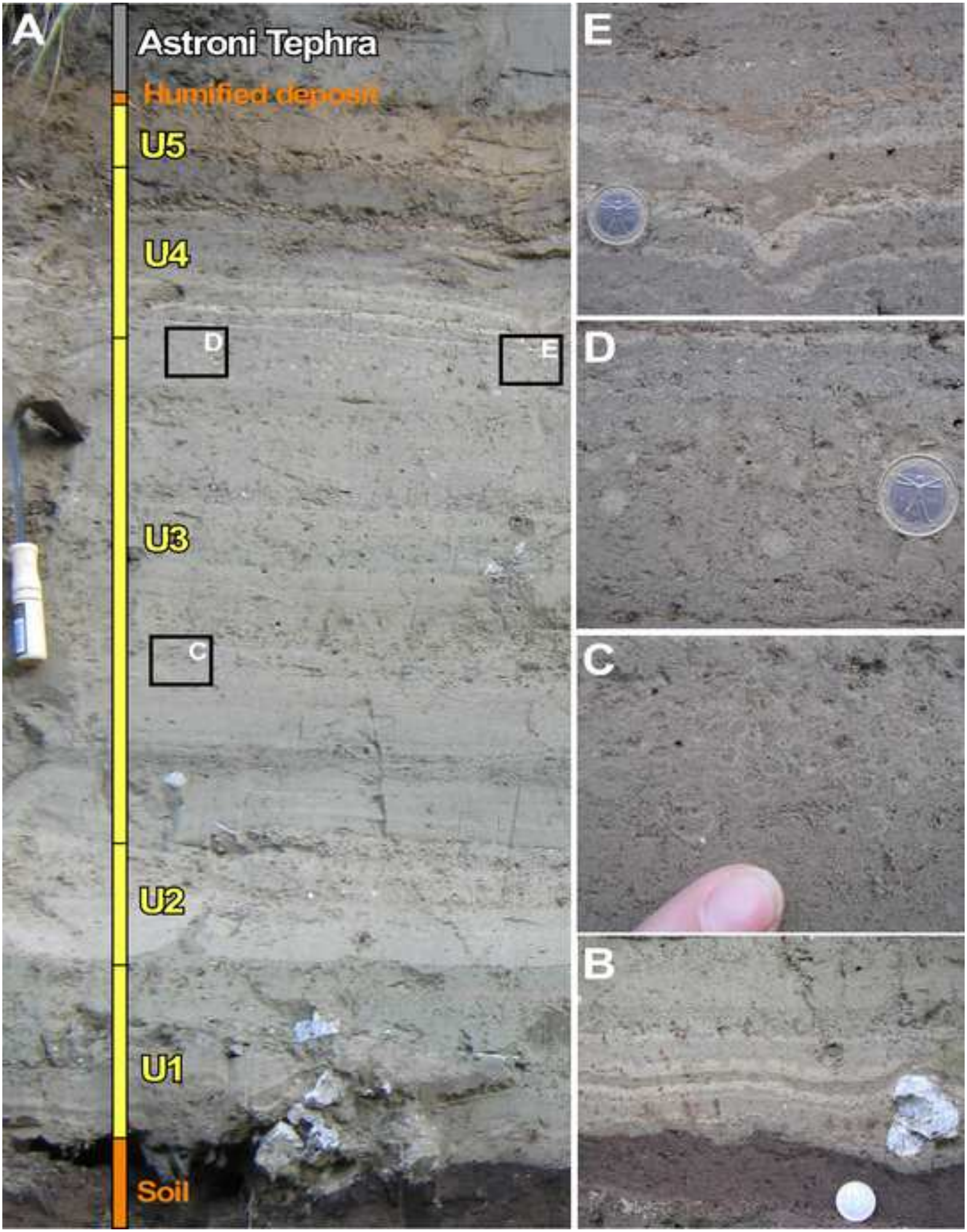
A
Astroni Tephra
Humified deposit
U5
U4
D
E
U3
C
U2
U1
Soil
E
D
C
B

Figure 2 Click here to download Figure Figure 2.tif

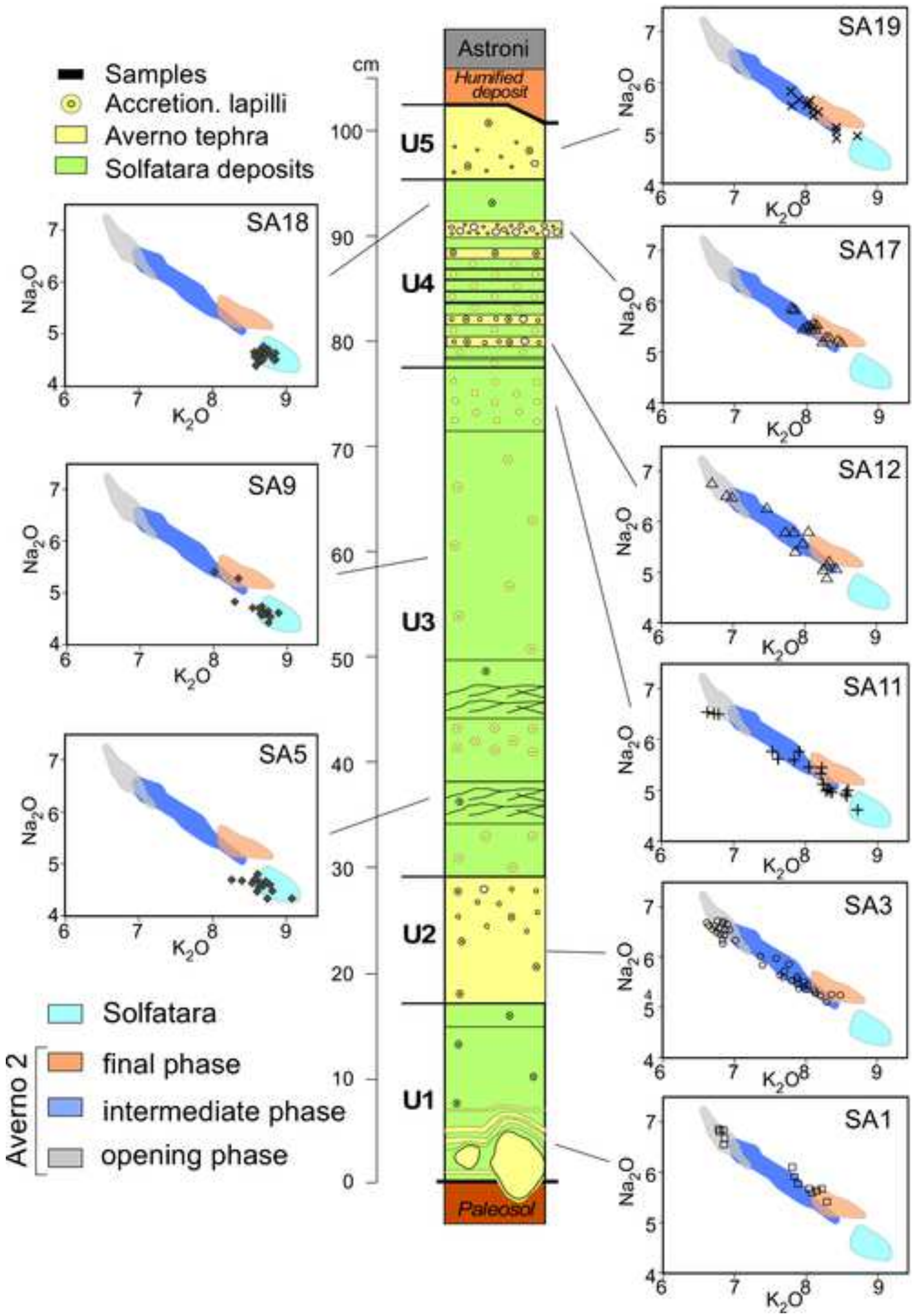

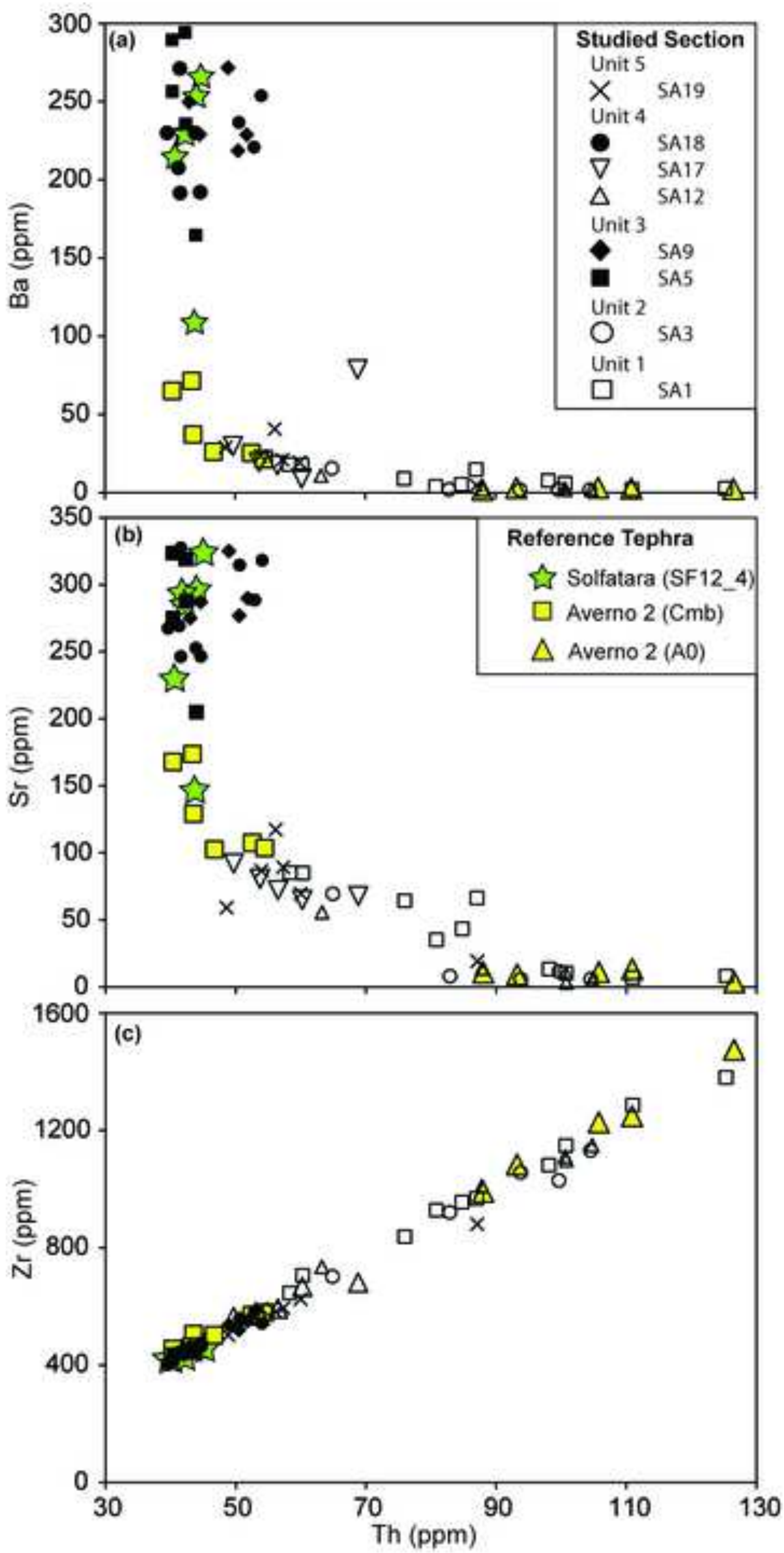
(a)
Studied Section
Unit 5
SA19
Unit 4
SA18
SA17
SA12
Unit 3
SA9
SA5
Unit 2
SA3
Unit 1
SA1
Ba (ppm)
(b)
Reference Tephra
Solfatara (SF12_4)
Averno 2 (Cmb)
Averno 2 (A0)
Sr (ppm)
(c)
Zr (ppm)
Th (ppm)

GSA Data Repository xxxxx

Simultaneous eruptions from multiple vents at Campi Flegrei (Italy) highlight new eruption processes at calderas

Marco Pistolesi, Roberto Isaia, Paola Marianelli, Antonella Bertagnini, Céline Fourmentraux, Paul G. Albert, Emma L. Tomlinson, Martin A. Menzies, Mauro Rosi and Alessandro Sbrana

METHODS

Nomenclature

The tephra sequence explored in this work has been divided into 5 main units (U1 to U5), mainly based on tephra sedimentological characteristics (color and grain-size variations), consisting of an alternation of accretionary lapilli-bearing, ash layers with scattered pumice fragments.

The Averno 2 tephra sequence has been divided (Di Vito et al., 2011; Fourmentraux et al., 2012), from base to top, into three Members, namely A, B and C. The lower part (Member A), has been divided in six fallout sub-members (A0 to A5) interlayered with thin, fine-grained surge deposits. A2 sub-member, which represent the climax of the eruption, has been further divided into a basal (A2b) and a top (A2t) layer. The intermediate part (Member B) consists in a complex sequence of surge bedsets intercalated with minor fallout deposits, with sample Bt representing one of the fallout bed of the upper portion of the member. Finally, Member C represents the final stage of the eruption mostly consisting in surge beds; Cmb represents a thin fallout bed within the lower portion of the member. For the sake of simplicity, we tried to preserve this existing nomenclature (Di Vito et al., 2011; Fourmentraux et al., 2012) by modifying it only to simplify unnecessary details. We divide the Averno 2 eruption into three main phases: i) opening phase (corresponding to Member A0 in Di Vito et al., 2011), ii) intermediate phase, which includes the peak fallout deposit (A2) followed by a PDC and minor fallout phase deposits (member B); iii) final phase (PDC and minor fallout deposits of Member C).

Field data collection

Field data collection was carried out during different surveys, which allowed detailed stratigraphic reconstructions of the two eruptions. Although stratigraphic sections in which the two eruptions are clearly intercalated are few, the work benefited from the years-lasting stratigraphic and petrological work on the reconstruction of the two single eruptions. In the stratigraphic survey, about 10 natural sections were investigated. At each site, a detailed stratigraphic log of volcanic succession was measured and described. All information (global positioning system [GPS] coordinates, photos and field notes) was stored in geographic information system (GIS) format, on a digital topographic base. Several tephra sections, where the deposits of the Averno and Solfatara eruptions are interlayered, were studied with joint field activities involving all the authors. Among these stratigraphic sections, one was particularly valuable thanks to its preservation and was selected for detailed sampling (33T 425942 4520976 UTM).

Two compositional end-members emitted during the opening and final phase of Averno 2 eruption were analyzed as reference samples. A0, representing the opening phase, was collected at La Torretta (33T 420909 4520782 UTM) while sample Cmb, representing pumice clasts19-cm thick fallout layers in the middle portion of member C were collected at La Schiana (33T 422613 4522150 UTM). The reference sample from the proximal Solfatara sequence (SF12_4) was collected on the northwestern side of the crater area (33T 426804 4520436 UTM).

Grain-size analyses

Collected samples were dry-sieved for grain-size analyses with a set of sieves with 0.5 phi (ϕ) interval from -6ϕ to fine ash particle (<6ϕ, where ϕ=-log diameter of the particle in mm) at Dipartimento di Scienze della Terra of Pisa (Italy). The presence of a significant amount of fine ash in most of the samples required the use of a laser particle size analyser (Mastersizer 2000, Malvern; CNR-ISE Pisa) on the finest fraction (<32 µm). Grain-size data are reported in Fig. DR4.

SEM-EDS analyses

Pumice fragments (including some accretionary lapilli) were separated from the -0.5ϕ (1.4–2 mm) and -2ϕ (4–5.6 mm) grain-size fractions, mounted on double-adhesive tape on a glass slide and embedded in epoxy resin for morphological scanning electron microscope (SEM) observations and energy-dispersive spectroscopy (EDS) analyses on residual glass. From the coarsest bed at the base of the section, 13 lapilli-sized clasts (from 2 to 6 cm) and one bomb (10 cm) were also analyzed. Analytical conditions were 20 keV accelerating voltage, 0.1 nA beam current and a working distance of 10 mm. We used a raster window of about 10×10 μm^2 to avoid Na migration under the electron beam during analysis. The analytical error is 1% for concentrations higher than 15 wt%, 2% for 5-15 wt%, 5% for 1-5 wt%, and 30% for <1 wt%. Before each session of analyses the quality of SEM EDS analyses was checked using CFA47 trachytic, ALV81R23 basaltic, and KE12 pantelleritic glasses as internal reference standards. Information about precision on each oxide, accuracy and standards used are reported in Table DR1, in which all EDS analyses are reported; in Fig. 2 only averaged data of multiple analyses collected on the same clast are reported.

LA-ICP-MS analyses

LA-ICP-MS analyses of the Solfatara and Averno samples were performed using a Thermo Scientific iCAP Qc ICP-MS coupled to a Photon Machines analyte 193 nm eximer laser ablation system with a Helix two-volume ablation cell at the department of Geology, Trinity College, Dublin. We used 36 and 30 µm laser spots, depending on the size of glass areas available for analysis in individual samples. The repetition rate was 5 Hz and the count time was 40s (200 pulses) on the sample and 30s on gas blank (background). Concentrations were calibrated using the NIST613 external standard with ^{29}Si as the internal standard. Data reduction was performed manually in Microsoft Excel allowing for the removal of signal compromised by microcryst inclusions. Full details are presented in Tomlinson et al. (2010). Accuracies of analyses of the ATHO-G and StHs6/80-G MPI-DING glasses are typically <5 %, standard data is presented in the supplementary material. Relative standard Errors (% RSE) for tephra analyses are typically <5 % for Y, Zr, Nb, La, Ce, Pr, Nd, Th and U; and <7% RSE for Rb, Sr, Ba, Sm, Eu, Dy, Er, Yb, Lu, Hf, Ta. Full errors (standard deviations and standard errors) for individual samples are presented in Table DR2.

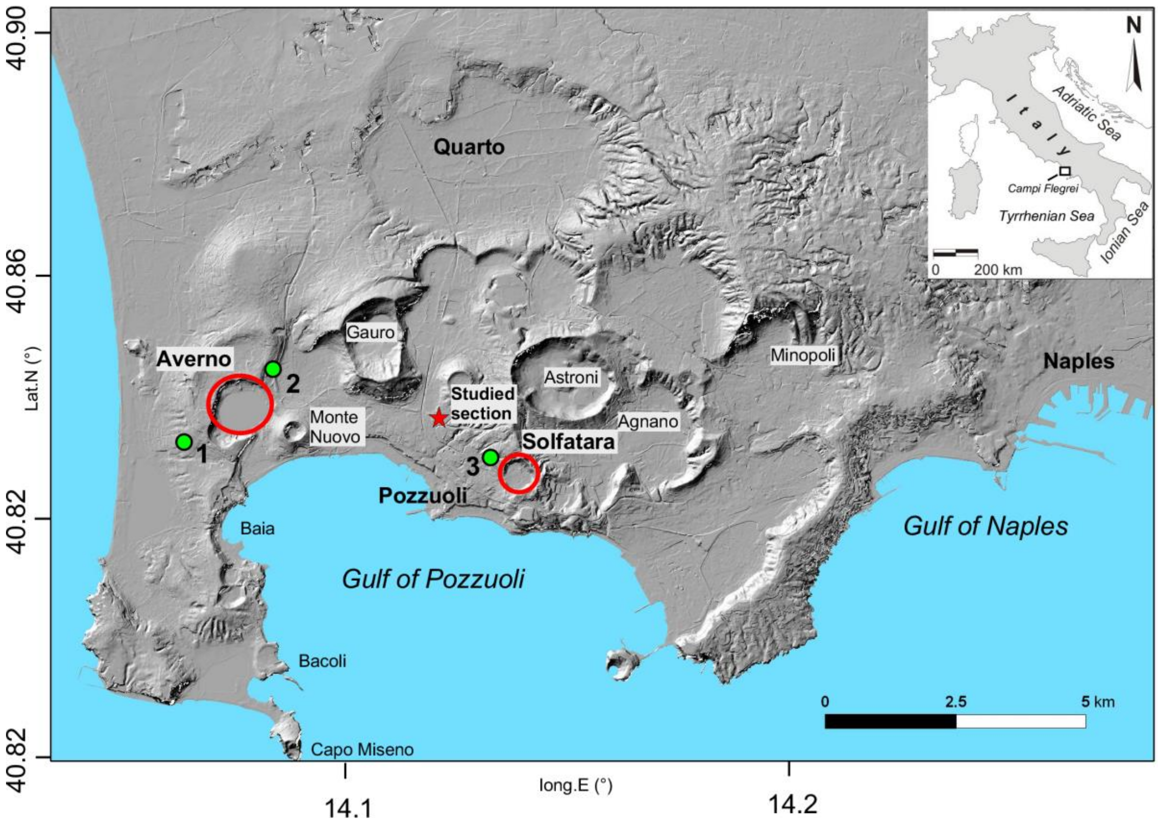

Figure DR1. Shaded relief map of the Campi Flegrei caldera with the Averno 2 and Solfatara volcanoes highlighted in red and the new studied stratigraphic section indicated by a red star. Green dots represent the locations of the reference samples for Averno 2 (1 – La Torretta; 2 – La Schiana) and Solfatara (3 – SF12_4).

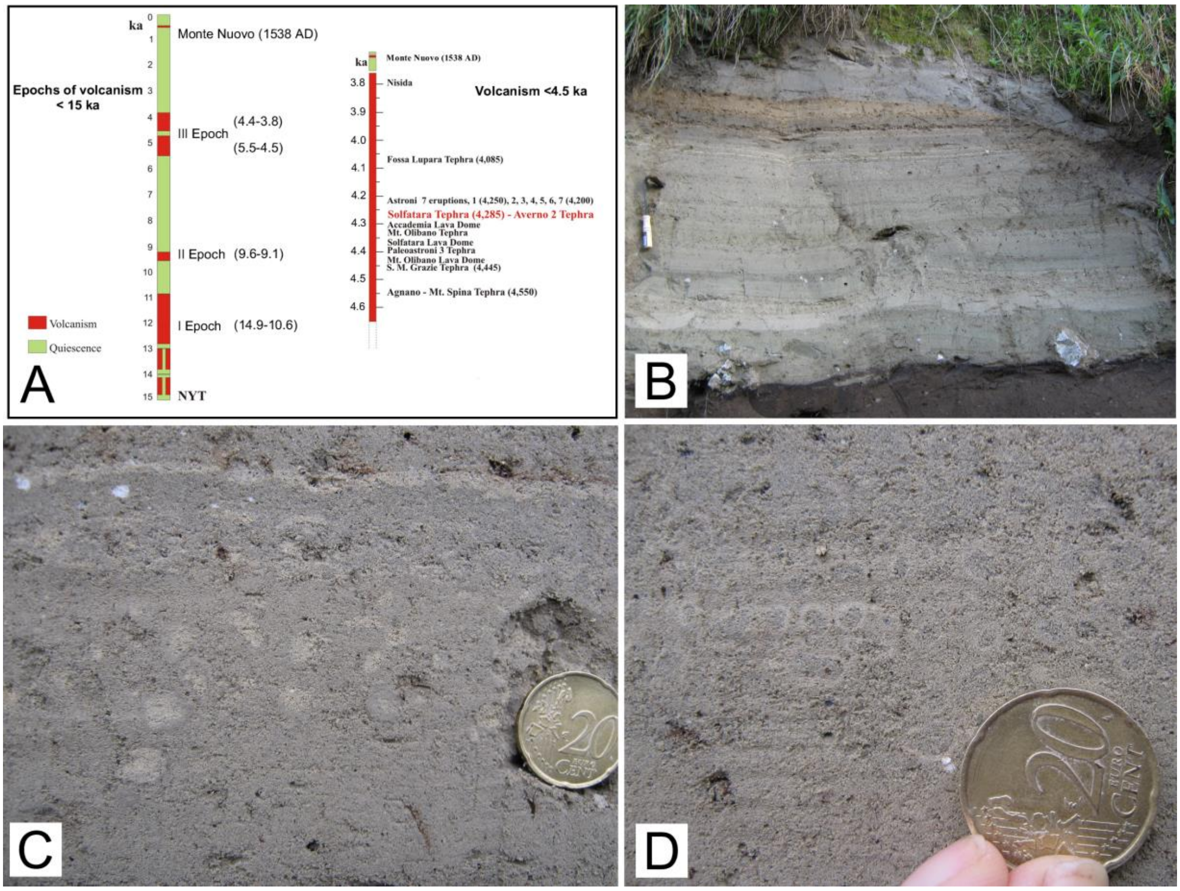

Figure DR2. (A) Chronostratigraphic section of volcanism younger than 15 ka at the Campi Flegrei caldera, and a detailed section for the volcanic events younger than Agnano Monte Spina (about 4.5 ka); modified after Isaia et al. (2009). (B) Solfatara-Averno 2 stratigraphic section studied in this work. Tool on the left for scale is 30 cm. (C, D) Details of the two types of accretionary lapilli found in Unit 3.

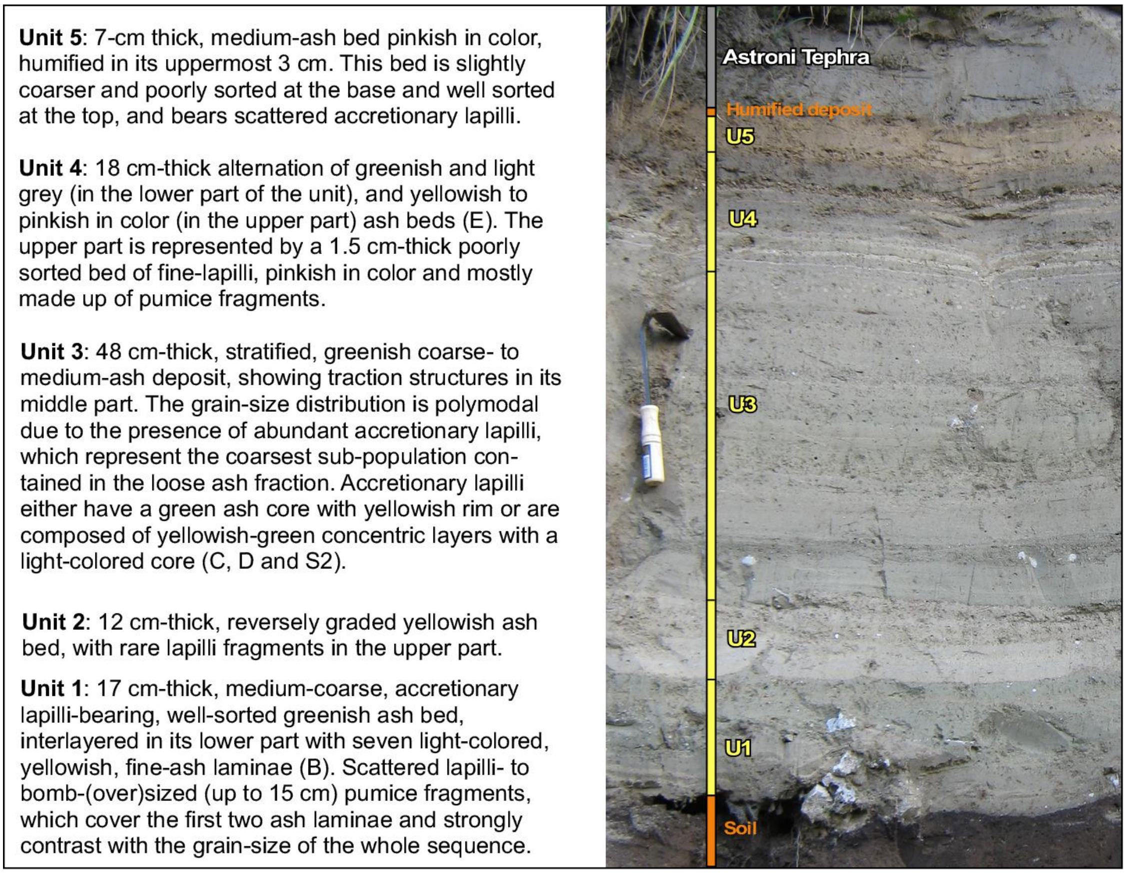

Figure DR3. The key section where Solfatara and Averno 2 deposits are interlayered. The main characteristics of each unit are described on the left.

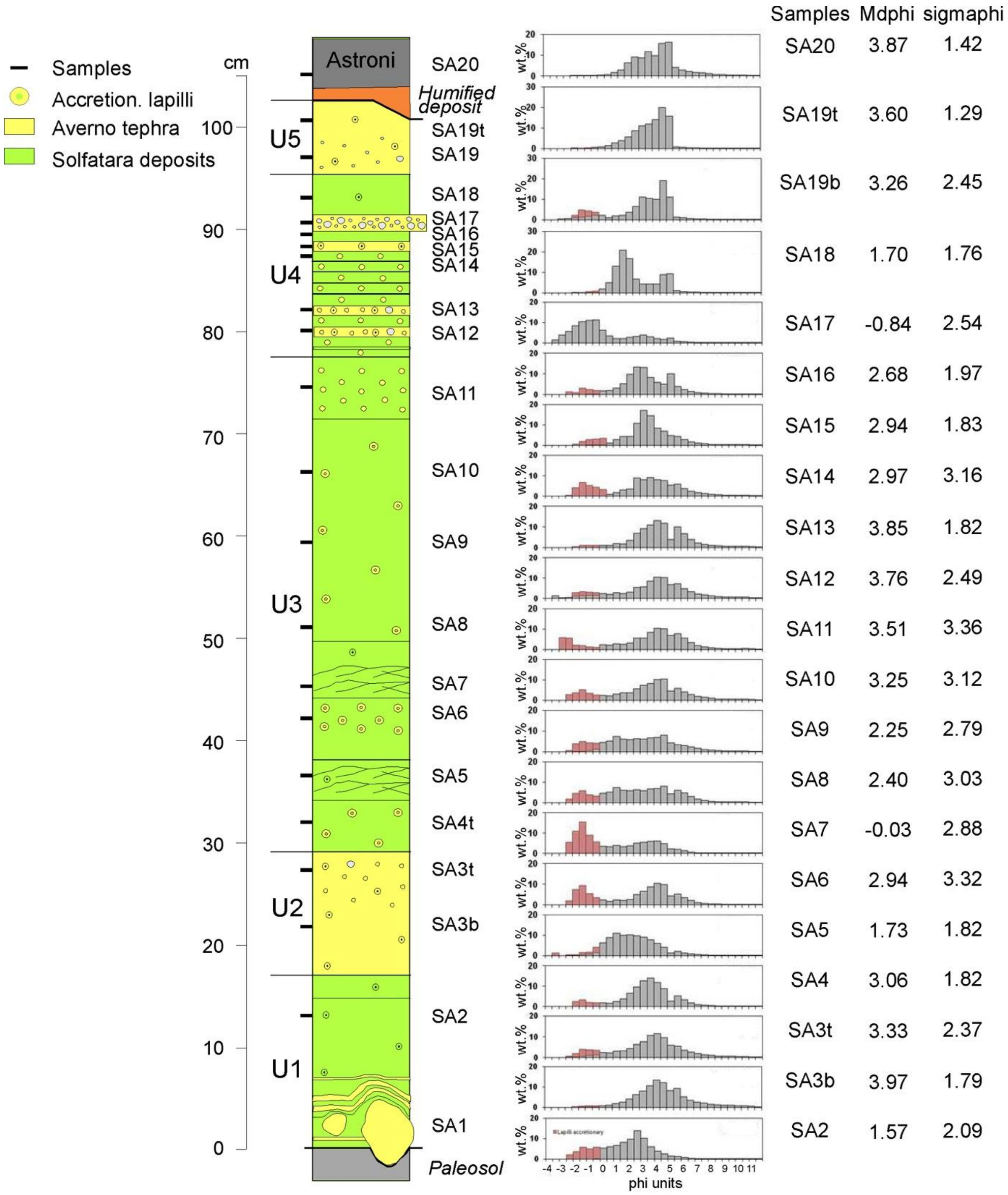

Figure DR4. Stratigraphic sequence with grain-size analyses of the collected samples. Pink bars in grain-size histograms refer to classes where accretionary lapilli were clearly identified.

Table DR1. SEM-EDS major analyses of the analyzed samples. Standards are also reported (separated .xls file).

Table DR2. LA-ICP MS trace elements of the analyzed samples. Standards are also reported (separated .xls file).

Table DR3. Timing of eruptive events and corresponding tephra units.

TABLE DR3. TIMING OF EVENTS AND CORRESPONDING TEPHRA UNITS

Unit	Solfatara	Averno
	Probably the Solfatara activity ends slightly before that of Averno	
U5	–	Last phase of the eruption (Member C)
U4	Ash fallout	Minor pumice fallout associated with PDC generation.
U3	Magmatic/phreatomagmatic phase, PDC generation, breccia and stratified ash deposits	Low level activity at the end of Member B phase. Two types of accretionary lapilli
U2	Pause between first and second phase	Ash-laden plumes during the emplacement of PDC deposits of Member B
U1	Explosivity mostly driven by hydrothermal fluids. Deposits with limited dispersal. Phreatic breccias close to the vent	Magmatic explosions. Eruptive columns up to 10 km. Pumice and bomb fallout. A2t interlayered with the upper part of U1
	The 2 eruptions begin almost simultaneously	

Additional references

Di Vito, M.A., Arienzo, I., Braia, G., Civetta, L., D'Antonio, M., Di Renzo, V., and Orsi, G., 2011, The Averno 2 fissure eruption: a recent small-size explosive event at the Campi Flegrei Caldera (Italy): Bulletin of Volcanology, v. 73, p. 295–320, doi:10.1007/s00445-010-0417-0.

Fourmentraux, C., Métrich, N., Bertagnini, A., and Rosi, M., 2012, Crystal fractionation, magma step ascent, and syn-eruptive mingling: The Averno 2 eruption (Campi Flegrei, Italy): Contributions to Mineralogy and Petrology, v. 163, p. 1121–1137, doi:10.1007/s00410-012-0720-1.

Isaia, R., Marianelli, P., and Sbrana, S., 2009, Caldera unrest prior to intense volcanism in Campi Flegrei (Italy) at 4.0 ka B.P: implications for caldera dynamics and future eruptive scenarios: Geophysical Research Letters, v. 36 L21303, p. 1-6, doi:10.1029/2009GL040513.

Tomlinson, E.L., Thordarson, T., Muller, W., Thirlwall, M., Menzies, M.A., 2010, Microanalysis of tephras by LA-ICP-MS — strategies, advantages and limitations assessed using the Thorsmork ignimbrite (Southern Iceland). Chemical Geology, v. 279 (3–4), p. 73–89.